THE JOURNAL OF BIOLOGICAL CHEMISTRY VOL. 283, NO. 12, pp. 7813–7822, March 21, 2008

Location and Orientation of Serotonin Receptor 1a Agonists in Model and Complex Lipid Membranes*[S]

Received for publication, September 6, 2007, and in revised form, January 2, 2008 Published, JBC Papers in Press, January 9, 2008, DOI 10.1074/jbc.M707480200

Jakob J. Lopez[‡] **and Mark Lorch**[§1]

From the [§]*Department of Chemistry, University of Hull, Hull, HU6 7RX, United Kingdom and the* [‡]*Institute for Biophysical Chemistry, J. W. Goethe University Frankfurt, 60438 Frankfurt, Germany*

Magic angle spinning (MAS) NMR has been used to investigate the location and orientation of five serotonin receptor 1a agonists (serotonin, buspirone, quipazine, 8-OH-DPAT, and LY-163,165) in single component model lipid and brain lipid membranes. The agonist locations are probed by monitoring changes in the lipid proton chemical shifts and by MAS-assisted nuclear Overhauser enhancement spectroscopy, which indicates the orientation of the agonists with respect to the 1,2-dioleoyl-*sn*-glycero-3-phosphocholine lipids. In the single component bilayer, the membrane agonists are found predominantly in the top of the hydrophobic chain or in the glycerol region of the membrane. Most of the agonists orient approximately parallel to the membrane plane, with the exception of quipazine, whose piperazine ring is found in the glycerol region, whereas its benzene ring is located within the lipid hydrophobic chain. The location of the agonist in brain lipid membranes is similar to the 1,2-dioleoyl-*sn*-glycero-3-phosphocholine lipid bilayers; however, many of the agonists appear to locate close to the cholesterol in the membrane in preference to the phospholipids.

Drug molecule interaction with lipid membranes is a critical factor governing its final activity, because it needs to negotiate its way through several membranes on the way to its receptor protein. In an effort to facilitate the design of drugs, water/octanol partitioning coefficients are often used. However, this simple two-phase model falls short of adequately describing the complexity of lipid/drug interactions. A lipid membrane is a chemically very diverse environment. Lipid headgroups are often charged and highly hydrated, and the interface between the headgroup and hydrophobic core of a membrane is typified by the presence of glycerol, carbonyl groups, and lower concentrations of water. It is only the very center of the membrane that is nonpolar and excludes water (1, 2).

Drug molecules tend to contain substituted aromatic groups that add further complications; steric effects exclude aromatic groups from the lipid chain region (3), whereas other attractive forces between the ring and lipid carbonyls draw the molecule to the interface between the chain and headgroup regions of the membrane (4, 5). Furthermore, any charged chemical groups will be excluded from the low dielectric environment at the center of the bilayer (2). Consequently, the mechanism by which a molecule partitions into lipid bilayers or crosses a biological membrane will be a complex interplay of many factors.

The majority of drug targets are membrane proteins. Hence the interaction of a drug with the membrane is crucial for its efficacy and involves several interesting aspects, such as its location probability profile across the membrane bilayer, its orientation, and its structure. A high location probability in a particular part of a membrane and its orientation with respect to the membrane normal could well be important to how the drug is presented to the binding site of the target protein (6).

Finally, it is now recognized that cholesterol-rich microdomains ("lipid rafts") form within cellular membranes (7). Certain chemicals have displayed an affinity for such domains (8), and it is quite possible that such domains could have an impact on receptor drug interactions.

Surprisingly little high resolution information exists on the location profiles of drug molecules in lipid bilayers. Recently, ^{1}H NMR and specifically magic angle spinning-assisted nuclear Overhauser enhancement spectroscopy (MAS-NOESY)[2] experiments have proved to be an ideal tool for investigating the location of small molecules embedded in lipid membranes, with atomic resolution (3, 9, 10).

In this study, solid state NMR techniques are applied to DOPC and brain lipid bilayers doped with five diverse 5-HT$_{1a}$ receptor agonists (serotonin, buspirone, quipazine, 8-OH-DPAT, and LY-165,163). These molecules represent a cross-section of available serotonin receptor 1a (5-HT$_{1a}$) agonists and have varying octanol/water partitioning coefficients and 5-HT$_{1a}$ binding constants (see Table 1). The artificial agonist interactions with membranes are of particular interest because they must cross the blood-brain barrier to access their target protein. Moreover, the natural binding site for serotonin on the 5-HT$_{1a}$ receptor is thought to be located within the membrane and is consequently accessible only to molecules that accumulate in the surrounding lipids (11).

We present high resolution MAS-NOESY data of doped DOPC membranes, which determine the agonist locations

* The costs of publication of this article were defrayed in part by the payment of page charges. This article must therefore be hereby marked "*advertisement*" in accordance with 18 U.S.C. Section 1734 solely to indicate this fact.

[S] The on-line version of this article (available at http://www.jbc.org) contains supplemental Figs. S1 and S2.

[1] Supported by a Research Councils UK academic fellowship. To whom correspondence should be addressed. Tel.: 44-1482-465687; E-mail: M.Lorch@hull.ac.uk.

[2] The abbreviations used are: MAS, magic angle spinning; NOESY, nuclear Overhauser effect spectroscopy; DOPC, 1,2-dioleoyl-*sn*-glycero-3-phosphocholine; HETCOR, heteronuclear correlation spectroscopy; 5-HT$_{1a}$, serotonin receptor 1a; DROSS, dipolar recoupling on-axis with scaling and shape preservation.

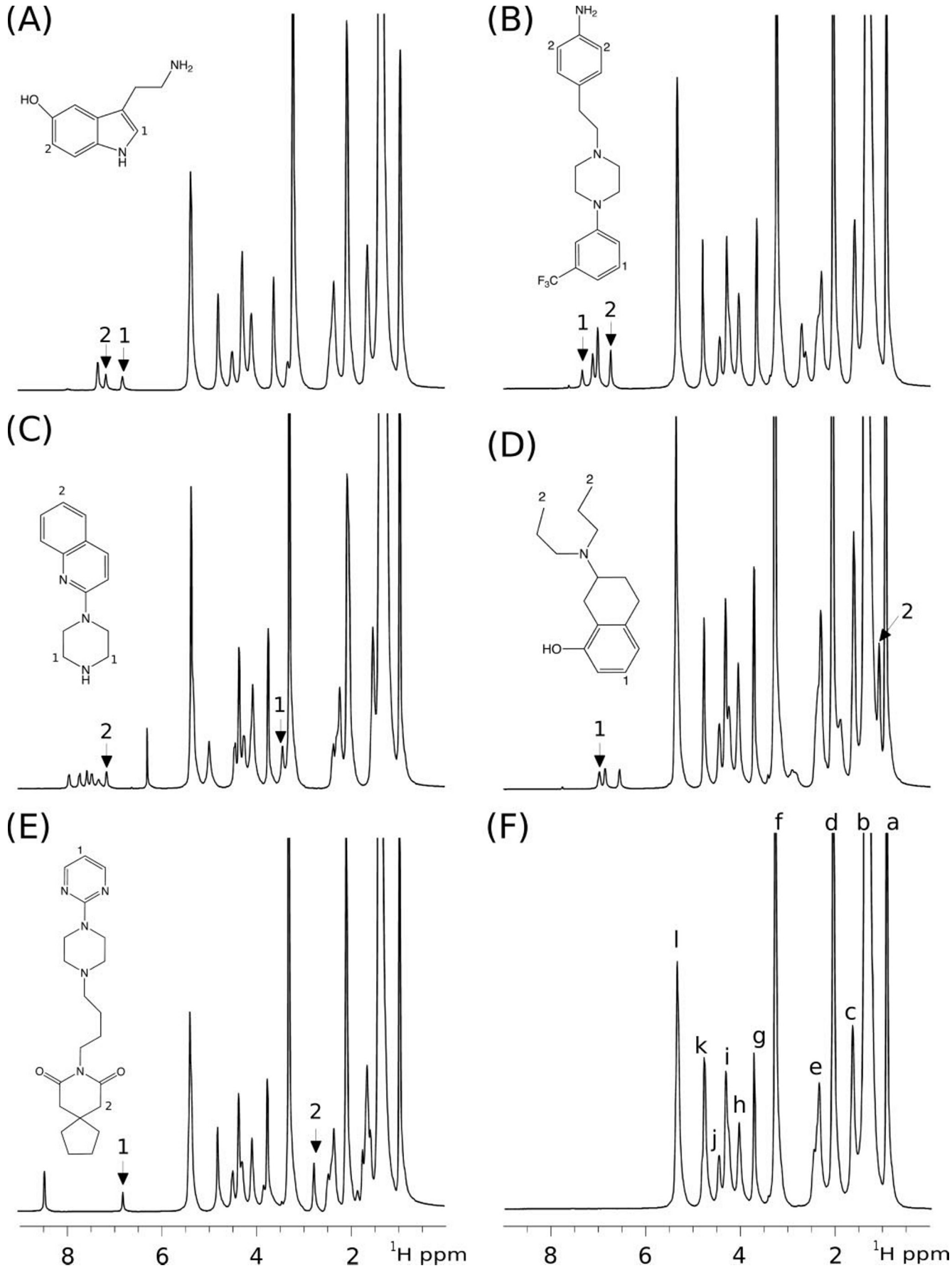
(A)
NH2
HO
1
2
N
H
2 1
(B)
NH2
2
2
N
N
F3C
1
1 2
(C)
2
N
N
1
1
1
N
H
2
1
(D)
2
2
N
HO
1
2
1
(E)
1
N
N
N
N
O
O
2
1
2
(F)
f d b a
l
k i
g
e
c
j
h
8 6 4 2 1H ppm
8 6 4 2 1H ppm

and orientation within the membrane bilayer. Chemical shift changes, induced by agonist aromatic rings in proximate lipid molecules, are used as a further indication of the drug molecules membrane coordinates. Interestingly, it was possible to show that the agonists preferentially interact with different components of the brain lipid systems.

EXPERIMENTAL PROCEDURES

Materials—1,2-Dioleoyl-*sn*-glycero-3-phosphocholine (DOPC) and porcine brain total lipid extracts were purchased from Avanti Polar Lipids (Alabaster, AL). The brain lipid extract consists of phosphatidylethanolamine (16.7% w/w), phosphatidylserine (10.6% w/w), phosphatidylcholine (9.6% w/w), phosphatidic acid (2.8% w/w), phosphatidylinositol (1.6%), and other (58.7% w/w) (Avanti Polar Lipids), of which the majority will be cholesterol (~30–40% w/w total lipid) (13). All other chemicals including serotonin, buspirone, quipazine, 8-OH-DPAT, and LY-165,163 were purchased from Sigma.

Sample Preparation—78 mg of DOPC and agonist was dissolved in chloroform/methanol (1:1 v/v) with a 4:1 lipid to agonist molar ratio. Brain lipid/agonist samples were prepared at the same ratios. The solvents were evaporated under vacuum, and the resulting lipid cake was suspended in 1 ml of doubly distilled water, frozen in liquid nitrogen, and then lyophilized overnight under high vacuum. The dry lipid mixtures were hydrated with ~20 μl of D_2O and then subjected to three freeze/thaw cycles. The mixtures were then transferred into 4-mm MAS rotors.

NMR Measurements—All NMR experiments (at 288 K) were carried out on a Bruker Avance II 500 MHz spectrometer using a 4-mm MAS probe operating at frequencies of 500.1025 MHz (^{1}H) and 125.7546 MHz (^{13}C). ^{1}H and ^{13}C experiments were carried out at 10 kHz (^{1}H) and 5 kHz (^{13}C) MAS speeds. ^{1}H and ^{13}C spectra were externally referenced to tetramethylsilane at 0 ppm.

^{1}H experiments were conducted with a typical $\pi/2$ pulse length of 7 μs and a relaxation delay of 4 s. Two-dimensional NOESY and correlation spectroscopy experiments had 256 or 512 increments and 8 or 16 scans/increment. NOESY build-up curves were acquired at mixing times of 0.01, 0.05, 0.1, 0.2, 0.3, 0.4, 0.6, and 0.8 s.

^{13}C spectra were collected with a typical $\pi/2$ pulse of 3.2 μs. Proton decoupling during the acquisition period was achieved using two pulse phase modulation (30 kHz). Two-dimensional ^{13}C-^{1}H heteronuclear correlation spectroscopy (HETCOR) measurements were typically carried out with 256 increments and 256 or 512 scans/increment. A recycle delay of 2 s was used for all ^{13}C-detected experiments. Lipid order parameters were determined by measuring ^{1}H-^{13}C dipolar couplings using two-dimensional dipolar recoupling on-axis with scaling and shape preservation (DROSS) experiments (14). ^{1}H-^{13}C dipolar couplings were extracted from the dipolar splittings directly from the spectrum. The splittings were converted to segmental order parameters as described by Warschawski and Devaux (15).

All of the NMR data were processed using Topspin version 1.3 (Bruker Instruments, Karlsruhe, Germany). NOESY peak volumes were obtained by peak fitting and integration using CARA (16).

Data Analysis—NOESY data were used to calculate the location of a given nucleus in the lipid membrane using the "full matrix rate analysis," described in detail by Huster *et al.* (17). In short, experimentally measured NOESY peak volume, represented by matrix A, at the mixing time t_m, and the cross-relaxation rate R are linked by the following matrix equation.

$$A(t_m) = A(0) \cdot \exp(-Rt_m) \quad \text{(Eq. 1)}$$

The relaxation rate matrix R is calculated by rewriting Eq. 1 as follows.

$$R = -\frac{X(\ln D)X^{-1}}{t_m} \quad \text{(Eq. 2)}$$

Here, X is the matrix of eigenvectors, and D is the diagonal matrix of eigenvalues of the normalized peak volume matrix $a(t_m) = A(t_m)[(A(0)^{-1}]$.

The relaxation rates, contained in R, were taken as indicators of the relative location probabilities and are plotted to give a location profile of the agonists, at atomic resolution.

All calculations were carried out with the help of Python 2.5, specifically with the modules pylab and SciPy (www.scipy.org).

RESULTS

The agonist to lipid ratio (1:4) used in this study is desirable to ensure good signal to noise of the NOESY cross-peaks and significant induced chemical shifts (see below). However, at these high agonist concentrations, measurements may be compromised by disruption of the lipid bilayer or agonist aggregation. Aggregation can be ruled out by the observation that agonist proton peaks are sharp and well resolved (Fig. 1, *A–E*), indicating that they are highly mobile. The line widths of the lipid proton signals are unaffected by the presence of agonist. It is well established that a change from a fluid lamellar to a gel phase is accompanied by a broadening of the NMR lines and subsequent loss of resolution (19, 20). Because no broadening is seen upon the addition of agonist (Fig. 1), it is safe to assume that the lipids, in all mixtures, remain in a fluid lamellar phase.

The phase of the lipids was further investigated by determining the order parameters of all DOPC/agonist mixtures. These values were extracted from ^{13}C-^{1}H dipolar couplings using a DROSS pulse sequence (14, 15) as opposed to the more well described ^{2}H measurements. The order parameters of all ago-

FIGURE 1. **^{1}H NMR spectra of DOPC/D_2O dispersion doped with 25 mol % of various 5HT$_{1a}$ receptor agonists.** *A–E*, DOPC/D_2O dispersions doped with serotonin, LY-165,163, quipazine, 8-OH-DPAT, and buspirone, respectively. The aromatic signals from the agonist can be seen between 6 and 8 ppm. The *insets* in *A–E* show the structures of the relevant agonists along with assignments for two of the NMR signals corresponding to protons on opposite poles of the molecule. *F*, DOPC without agonist. Assignments of the lipid signals are according to Yau *et al.* (3) and correspond to the labels on the lipid molecule in Fig. 4. *Peak a*, ω; *peak b*, chain CH_2(n); *peak c*, C-3; *peak d*, C-8 and C-11; *peak e*, C-2; *peak f*, γ; *peak g*, β; *peak h*, G-3; *peak I*, α and G_1; *peak j*, G_1; *peak k*, HDO; *peak l*, C-9, C-10, and G_2.

nist/DOPC mixtures (supplemental Fig. S1) are entirely consistent with previously published figures of fluid lamellar lipids, determined using the same DROSS sequence (14, 15). It should be noted that the order parameters derived from ^{2}H NMR experiments are systematically larger than those from DROSS measurements (15).

One-dimensional ^{1}H MAS NMR on Membranes Doped with Agonist—Proton MAS spectra of DOPC lipid membranes in the presence and absence of 5HT$_{1a}$ receptor agonists are shown in Fig. 1. Assignments of the agonist signals were carried out on the lipid/agonist mixtures using MAS-correlation spectroscopy (data not shown) and MAS-NOESY experiments. Full ^{1}H NMR assignments were performed. However, for the sake of simplicity, only two signal assignments for each agonist (one for each pole of the molecule) will be used for the analysis.

^{1}H NMR assignments for 1-palmitoyl-2-oleoyl-*sn*-glycero-3-phosphocholine determined elsewhere (3) were used for the assignment of the DOPC signals. Although most DOPC proton resonances are resolved (Fig. 1*F*), it is worth noting that, of the two G_1 proton signals, one overlaps with the headgroup α protons peak. In the following, the isolated peak at 4.49 ppm will henceforth be referred to as the G_1 signal.

^{1}H MAS NMR spectra of the brain lipid membranes are, in general, more convoluted than DOPC spectra. This is due to the higher complexity in composition of the membrane (see "Materials"). Broad lines and a narrow chemical shift dispersion result in numerous overlapping resonances (data not shown).

^{1}H NMR signals of the agonist aromatic moieties (Fig. 1, *A–E*) are well resolved and downfield of the lipid resonances (>6 ppm). Aliphatic agonist signals overlap with the stronger lipid signals, with the exception of CH_3 protons of 8-OH-DPAT (Fig. 1*D*, *resonance 2*), CH_2 protons in the piperazine ring of quipazine (Fig. 1*C*, *resonance 1*), and CH_2 protons in the cyclopentane ring of buspirone (Fig. 1*E*, *resonance 2*).

The presence of agonists in the lipid membrane causes shifts in the lipid proton signals, because of the aromatic ring current effect (3, 10, 21). The strength of the effect rises with the proximity of the drugs aromatic rings to the lipid proton, whereas its sign is dependent on the orientation of the ring relative to the lipid proton. An analysis of these effects can indicate an average location and orientation of the aromatic rings of an agonist relative to the lipid molecules.

All agonists induce significant shifts in the lipid signals (Fig. 2), most notably in between the top of the alkyl chains and the headgroup. Serotonin and LY-165,163 cause large shifts of the lipid headgroup resonances. All of the artificial agonists also cause large shifts to the C-2 and C-3 protons. Serotonin, buspirone, 8-OH-DPAT, and quipazine have very little or no effect on the protons in the remainder of the lipid chain. LY-165,163 is the only agonist that causes a significant shift in all signals throughout the alkyl chain region, but like the other molecules it has the largest effect on the C-2 and C-3 protons.

In the DOPC membranes, all of the shifts are upfield (with the exception of a small downfield shift in the G-3 protons of serotonin-doped bilayers), indicating that the average location of the lipid protons is above the agonist rings. These observations are in good agreement with similar studies where the presence of tryprophan (3) and flavonoid analogs (10) produced exclusively upfield shifts.

MAS-NOESY Measurements on DOPC Membranes Doped with Agonist—A typical MAS-NOESY spectrum of serotonin in DOPC membranes is depicted in Fig. 3. Cross-peaks are visible between all aromatic serotonin and DOPC resonances. The build-up rates of the cross-peaks with increased mixing times give an indication of the proximity of two protons (supplemental Fig. S2). Consequently, the location probability of a particular agonist proton in the lipid membrane can be determined relative to other agonist protons. If multiple agonist proton signals are resolved (Fig. 1), the orientation of the molecule in the membrane may be determined as well.

In general the maximum location probability for all aromatic protons is located between the headgroup and alkyl chain regions of the membrane (Fig. 4). Maximum peak intensities for all aromatic resonances are found between positions C-3 and G-3 of the lipid chain, in agreement with similar studies of aromatic molecules in lipid membranes (3, 9, 10).

Quipazine and LY-165,163 show markedly different behavior (Fig. 4, *B* and *C*). One end of the quipazine molecule has intense cross-peaks occur between the aromatic ring protons and the C-8 and C-11 groups situated half-way down the lipid chain. However, like the other agonists, very small cross-peaks are seen with the ω-CH_3 group at the end of the lipid chain. LY-165,163 has significant cross-relaxation rates with the whole of the lipid molecule but with the maximum still between the C-3 and G-3 positions in the lipid chain. (Fig. 4*B*).

Proton signals from opposite ends of the agonists indicate the interaction with different parts of the lipid molecules. The majority of the agonists shows only mildly different patterns of cross-peak intensities for either end of the molecule.

In the case of serotonin, the ends of the molecules have a maximum location probability in the glycerol region of the membrane. The aromatic ring, however, has a distribution that is located closer to the top of the alkyl chain, whereas the pyrrole ring tends toward the headgroup (Fig. 4*A*).

The aromatic ring of 8-OH-DPAT has a strong preference for the top of the alkyl chain, whereas its CH_3 groups have a broad distribution stretching from the lipid C-3 group to the β CH_2 in the headgroup (Fig. 4*D*). This would suggest that the alkyl chains of DPAT are highly mobile and do not have a strong location preference.

Both the aromatic and isopentane groups of buspirone have location maxima in the glycerol region. However, the isopentane also has a significant cross-peak with the α-CH_2 protons in the lipid headgroup (Fig. 4*E*), suggesting that buspirone has an angled orientation, with the isopentane group located higher in the membrane than the aromatic group.

The strongest orientation bias is exhibited by quipazine; the aromatic ring is buried well within the hydrophobic chain, and the piperazine ring has a strong preference for the glycerol region (Fig. 4*C*). As a result quipazine appears to adopt an orientation parallel with the lipids.

Most interestingly one end of LY-165,163 has two location maxima. The trifluoromethylbenzene ring has a clear location centered on the top of the lipid alkyl chain. However, the aniline

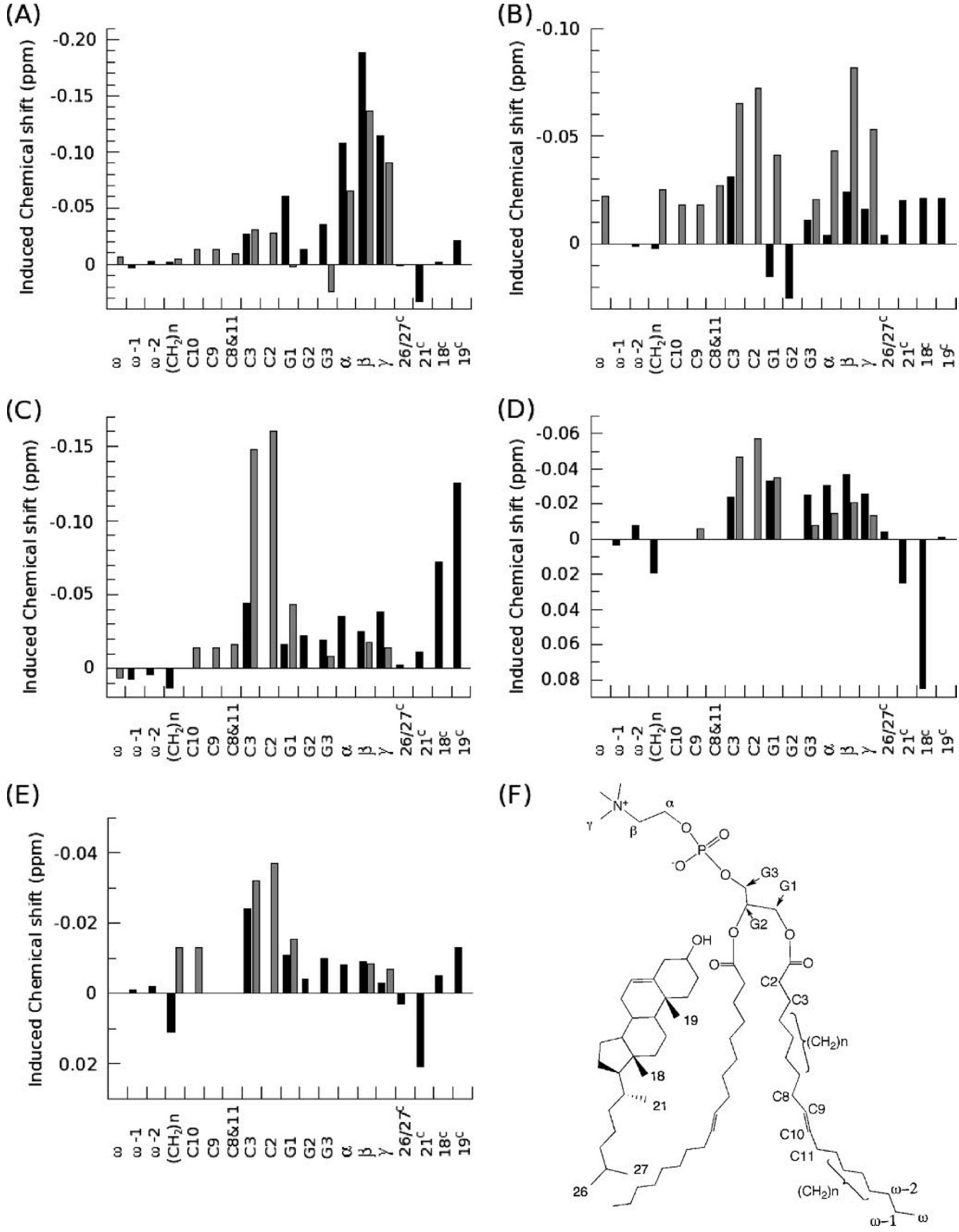

FIGURE 2. **Aromatic ring current induced chemical shifts of agonists in DOPC (*gray*) and brain lipid (*black*) bilayers for serotonin (*A*), LY-165,163 (*B*), quipazine (*C*), 8-OH-DPAT (*D*), and buspirone (*E*).** DOPC data are derived from one-dimensional proton MAS measurements. The brain lipid data are derived from ^{13}C-^{1}H correlation measurements. *F* shows resonance assignments for cholesterol and DOPC.

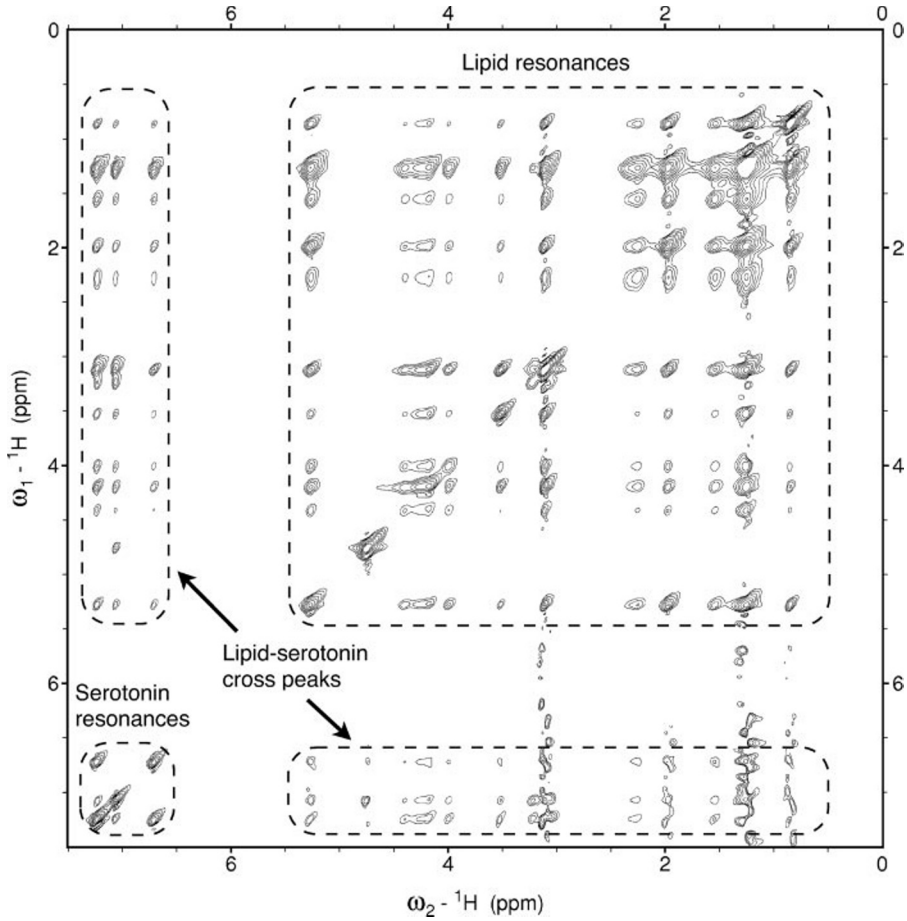

FIGURE 3. **Two-dimensional ^{1}H MAS NMR NOESY spectrum of DOPC membranes doped with serotonin.** The lipid signals can be seen between 0 and 6 ppm. The aromatic signals from serotonin are between 6 and 8 ppm and are well separated from the lipid signals. The cross-peaks between lipid and serotonin signals give the location of the serotonin in the membrane.

ring, at the opposite end of the molecule has two location maxima, one in the lipid head group and the other in the lower alkyl chain region (Fig. 4*B*).

It should be noted that signals from agonist methylene groups overlapping with the lipid signals may contribute to cross-peak intensities. However, MAS-NOESY measurements carried out at lower agonist concentrations (1:10 molar ratio) (data not shown) resulted in similar distribution profiles, indicating that this source of error is not of concern.

Two-dimensional ^{13}C MAS NMR on Brain Lipid Membranes Doped with Agonist—^{13}C-detected NMR experiments offer increased resolution over proton-detected experiments (Fig. 5*A*). By extending the ^{13}C measurements into a second dimension, using HETCOR measurements, ^{13}C chemical shifts may be correlated with the chemical shifts of covalently bonded protons (Fig. 5*B*). The extra resolution of ^{13}C measurements now resolves individual proton resonances in the crowded spectra of brain lipid membranes. The HETCOR spectra are further simplified because quaternary ^{13}C nuclei, with no bonded ^{1}H nuclei, do not appear in the spectrum.

^{13}C lipid resonance assignments were based on previously published MAS NMR studies (22) and confirmed by one-dimensional ^{13}C spectra of DOPC and DOPC/cholesterol mixtures (data not shown). Phospholipid ^{13}C and ^{1}H signals of the alkyl chain and glycerol groups and phosphocholine and headgroups were assigned. The C-2 protons were not resolved in all brain lipid/agonist mixtures. Furthermore, the position of the alkene groups in the chains of brain lipids are variable and not good indicators of membrane location. Consequently, protons on the C-2, alkene groups, and carbons neighboring the alkene groups were omitted from use in the analysis of brain lipid data.

Signals corresponding to the CH_3 groups of cholesterol were easily resolved and assigned, because of their high signal intensities, compared with other CH groups (Fig. 5*B*). Many signals arising from the remaining cholesterol resonances and other components of the membrane were left unassigned. However, enough reliable assignments exist for a comparison between the neat DOPC lipid bilayers and the brain lipids.

As found for experiments with bilayers consisting of neat DOPC lipids, introducing agonists to brain lipid bilayers causes changes in lipid proton chemical shifts. The magnitude of the peak shifts is illustrated in Fig. 6, where peak shifts are induced by the presence of serotonin (Fig. 6, where peaks without serotonin are *black*, and those with serotonin are *blue*). These results are summarized in Fig. 2, where they are directly compared with the induced chemical shift data in the DOPC measurements reported above.

Overall, the agonist-induced chemical shifts on phospholipid protons in brain lipids indicate similar effects to those seen in pure DOPC membranes; only very small shift changes occur in the alkyl chain region of the membrane, larger changes are seen for the interface and phosphocholine headgroup resonances (Fig. 2). The only notable differences between the induced chemical shifts changes in brain lipids as compared with DOPC membranes occur with quipazine (Fig. 2*C*) and LY-163,165 (Fig. 2*B*) doped membranes. For the latter, the C-3 protons no longer experience shift changes significantly greater than other headgroup or interfacial protons, whereas for LY-163,165 doped brain lipid membranes, the alkyl chain below the C-3 group does not undergo any induced chemical shifts. It is worth noting that in brain lipid membranes more protons are shifted downfield by the presence of agonist. This is particularly evident in the glycerol region of LY-163,165 doped membranes (Fig. 2*B*) and in the alkyl chain region of quipazine, 8-OH-DPAT, and buspirone doped membranes (Fig. 2, *B* and *C*). Although

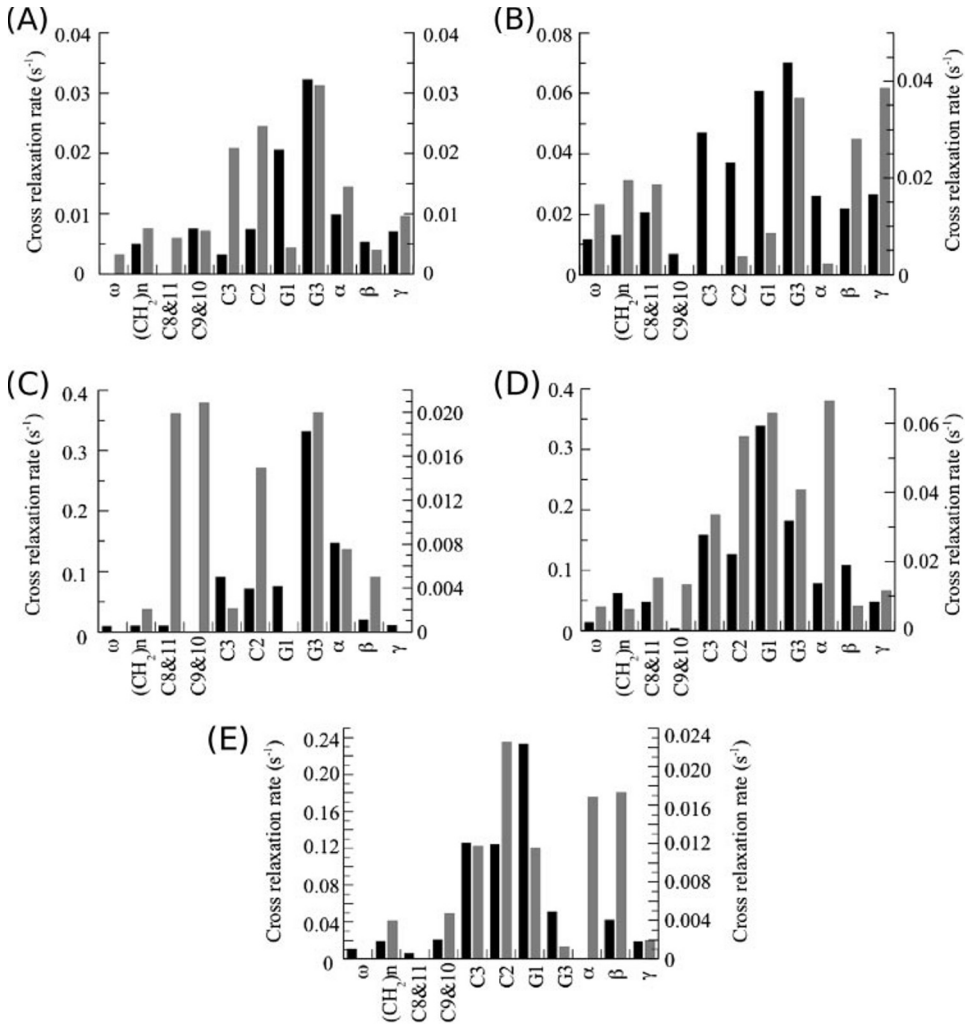

FIGURE 4. **Cross-relaxation rates between DOPC and agonists derived from MAS-NOESY measurements for serotonin (*A*), LY-165,163 (*B*), quipazine (*C*), 8-OH-DPAT (*D*), and buspirone (*E*) in DOPC bilayers.** *Black* and *gray bars* represents positions 1 and 2 of each agonist as defined in Fig. 1, respectively. *Black bars* use the *left axes*, and *gray bars* use the *right axes*.

the downfield shifts are minor (<0.02 ppm), their presence is significant, because downfield shifts are largely absent from the DOPC doped membranes, nor are they seen in comparable studies of doped single component membranes (3, 10).

Well resolved cholesterol proton signals enable the extraction of information on the interactions between the sterol and agonists (Fig. 5*B*). The induced chemical shifts experienced by the cholesterol protons follow the same pattern as the phospholipid protons. The smallest changes are experienced by the groups situated closest to the bilayer center. Interestingly, agonists often cause comparable and in two cases larger shifts in the cholesterol protons than the phospholipid protons. This is especially noticeable for quipazine and 8-OH-DPAT doped membranes, where the magnitude of the cholesterol-induced chemical shifts is two to three times that experienced by the phospholipids protons (Fig. 2, *C* and *D*).

A striking exception to the upfield (or small downfield) shifts was observed for cholesterol in the 8-OH-DPAT doped brain lipid membranes (Fig. 2*D*). Both the 21c and 18c protons experienced downfield shifts, where the 18c shift change was particularly pronounced (~0.08 ppm).

DISCUSSION

This work compares the locations of 5-HT$_{1a}$ receptor agonists in neat component membranes and multicomponent brain lipid membranes. The data give an indication as to how the membrane environment affects the way agonists may be delivered and presented to target proteins.

The NOESY data show that the majority of the agonists have the highest location probability within the interface between the chain and headgroup regions. Furthermore, the agonist molecules lie with their long axis approximately parallel to the membrane plane (data summarized in Fig. 7).

Quipazine is located deeper in the membrane (the quipazine benzene ring has its highest location probability in the upper alkyl chain region) and has a strong orientation bias that puts it perpendicular to the membrane plane.

Interestingly LY-165,163 has an unusual location behavior. It has a significant population throughout the whole lipid bilayer, and the aniline ring has two location maxima at opposite ends of the lipid chain.

The agonist aromatic rings alter the surrounding chemical environment, which manifests itself as a change in the chemical shift of proximate lipid proton NMR signals and provides a second indication for measuring the molecules location in the membrane. These induced chemical shift data, for both DOPC and brain lipids, broadly agree with the NOESY data; the agonists preferentially locate between the top of the alkyl chain and the choline headgroup.

Some features of the induced chemical shift data are worth further discussion. First, the glycerol proton resonances experience very small agonist-induced chemical shifts, despite the fact that the NOESY data place the location of the agonists squarely in this region of the bilayer. Similar studies (with indole derivatives) (3) reported the same discrepancies between chemical shifts and NOESY data. This is likely to be due to the tight packing in this part of the membrane along with the proximity of lipid carbonyl group shielding, which produces a similar chemical environment to the agonist aromatic rings (23). Hence, the presence of the agonist does not cause a significant change in the glycerol proton environment, making glycerol protons insensitive to aromatic induced chemical shifts. As a

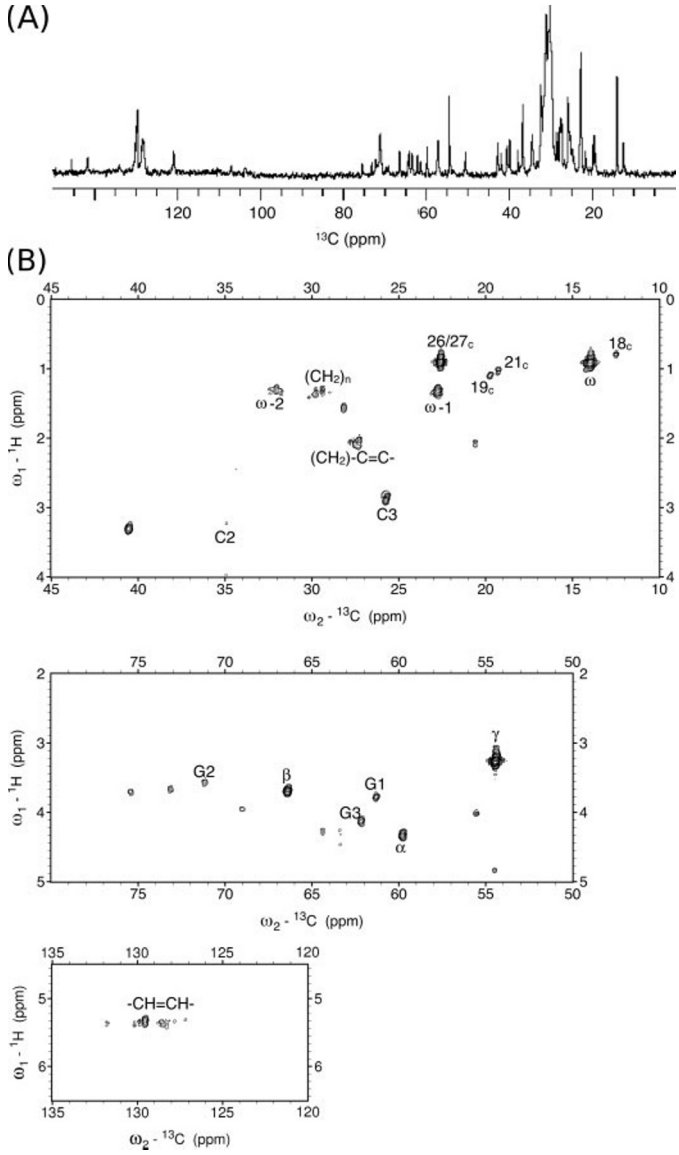

FIGURE 5. **^{13}C-detected NMR spectra.** *A*, one-dimensional ^{13}C proton decoupled MAS. *B*, two-dimensional ^{1}H-^{13}C HETCOR correlation experiment for brain lipid membranes. Pure brain lipids with assignments are shown, and the *subscript c* denotes cholesterol resonances. Unlabeled resonances cannot be confidently assigned.

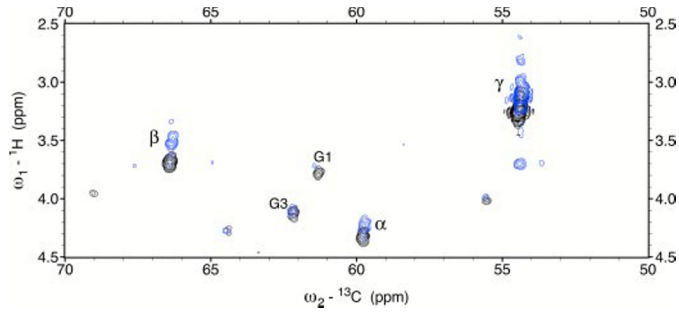

FIGURE 6. **HETCOR spectra showing the headgroup and glycerol resonances from pure brain lipids (*black*) and brain lipids doped with serotonin (*blue*).** The induced proton chemical shifts caused by the presence of serotonin can clearly be seen. The assignments of the peaks are shown.

result, the induced chemical shifts of the glycerol resonances may under-represent the concentration of agonists in this part of the membrane.

Serotonin induces large chemical shifts in the choline proton resonances of both DOPC and brain lipid bilayers. This is likely due to the water-soluble serotonin located in the aqueous phase surrounding the highly hydrated headgroup.

Interestingly, the artificial agonists interact with the cholesterol in the brain lipid membrane to a similar or greater extent than with phospholipids. This has implications for the accumulation of the molecules in a membrane. Cholesterol is a major component of some lipid microdomains (7). The fact that agonists cause a significant change in the chemical environment around the cholesterol implies that they may preferentially partition into lipid rafts. This may indicate how agonists cross the blood-brain barrier, especially because it is well established that ceramides (another component of lipid rafts) can modulate the permeability of lipid membranes to small solutes, dyes, and even proteins (24).

More information on the interaction between cholesterol and the agonists can be extracted from the sign of the induced chemical shift changes. Quipazine and LY-163,165 both cause exclusively upfield shifts, indicating that the cholesterol protons are located above the plane of the agonists' rings. The cholesterol 18c and 19c CH_3 protons stick up and out of the plane of the sterol rings, whereas the 21c CH_3 protons branch out of the cholesterol alkyl chain. To achieve the upfield shifts, quipazine and LY-163,165 must roll around the cholesterol molecule. In contrast serotonin and buspirone cause a downfield shift in protons on the alkyl chain and upfield shifts in the CH_3 groups substituted into the sterol rings. These results can be explained if the plane of the agonist rings stack below the sterol CH_3 groups, whereas the mobile alkyl chain samples the space at the edge of the agonists' rings. Unlike the other agonists, 8-OH-DPAT causes downfield shifts in both CH_3 groups on both the sterol ring and alkyl chain. This would seem to imply that it sits alongside and in plane with the sterol ring. It would therefore seem that although the agonists all interact (to a greater or lesser extent) with cholesterol, they do so in quite different ways, resulting in variable orientations relative to the cholesterol.

The interfacial location of the agonists tested here may appear at odds with the fact that the synthetic agonists are all hydrophobic, as their water-octanol partitioning coefficients (Table 1) would indicate. However, it has been demonstrated numerous times that aromatic ring structures do not penetrate into the chain region of lipid membranes (3, 9, 21). This has been attributed to numerous factors, including the entropic cost associated with intercalating a rigid ring structure into the mobile chain region (3), the fact that asymmetric aromatic molecules have dipole moments that cannot easily be accommodated in the nonpolar chain region of the lipid membrane (25), and the enthalpic requirements of hydroxy, carbonyl, and other substitutions on the ring to fulfill their hydrogen bonding potential (26, 27) (which cannot be achieved in the lipid chain region). Furthermore, bonding interactions between the π electrons of the lipid carbonyl group and aromatic rings (4, 5) may serve to anchor the agonists in the interface region (3, 10). The resulting interplay between the hydrophobic effect that drives the molecules into the hydrophobic core and a gamut of other

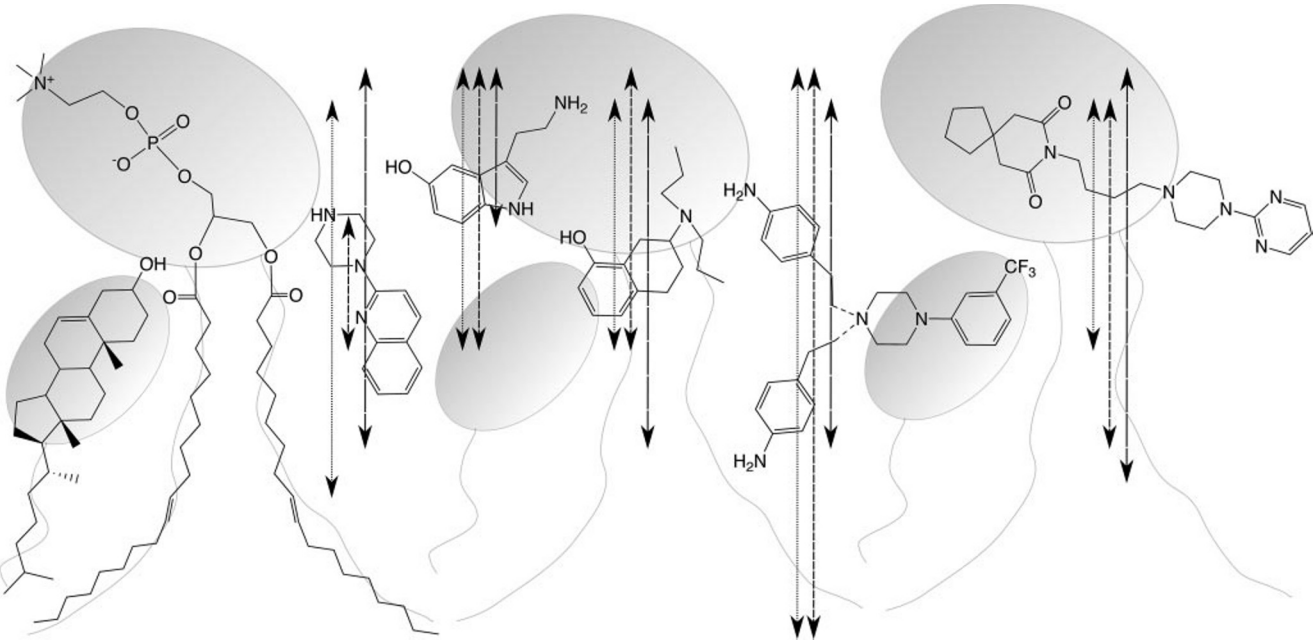

FIGURE 7. **Approximate location and orientation of 5HT$_{1a}$ agonists and cholesterol in lipid membranes.** The position of the cholesterol is as reported in the literature (12, 32). The position and orientation of each agonist is derived from maximum location probabilities extracted from NOESY data. The *arrows* represent the range over which a significant amount of agonist is found (>20% of the maximum induced chemical shift or cross relaxation rate) according to NOESY (*dotted line*), induced chemical shift of DOPC signals (*line with short dashes*), and brain lipid signals (*line with long dashes*). The two possible locations of the LY-165,163 aniline ring are show connected to the rest of the agonist by a *broken line*.

TABLE 1

Octanol/water partitioning coefficients and (Log P$_{ow}$) association constants (K_i) for 5-HT$_{1a}$ agonists

The average octanol/water partitioning coefficients (Log P$_{ow}$) were calculated using alogps 2.1.

Molecule	Average Log P$_{ow}$	K_i 5-HT$_{1a}$
		nM
Serotonin	0.62	2.2 (28)
Buspirone	2.72	15 (28)
Quipazine	2.26	780 (28)
8-OH-DPAT	4.2	1 (28)
LY-165,163	4.2	1.26 (29)

factors forces them to locate in hydrated regions of the membrane.

An important factor governing bioefficiency is the ability of the agonist to access the protein-binding site. To do this most efficiently, it must accumulate in the membrane close to the binding site and be presented to the protein in the correct orientation. Serotonin, 8-OH-DPAT, and buspirone accumulate in much the same region of the membrane and with similar orientations, whereas LY-165,163 is much more evenly distributed through the membrane. Quipazine is the only agonist that is oriented perpendicular to the membrane plane. It is therefore striking that, of the agonists tested here, quipazine has by far the lowest affinity for the 5-HT$_{1a}$ receptor. Most of the agonists have low nanomolar dissociation constants (28, 29) (Table 1) compared with 780 nM for quipazine (28). Quipazine orientation and location may go some way to explain its apparent lower affinity for 5-HT$_{1a}$. It may be that the preferred location and orientation of quipazine makes it inaccessible to the protein-binding site.

A further factor affecting the bioefficiency of an agonist will be its preference for particular microdomains within a membrane. It is becoming clear that some proteins preferentially locate in particular microdomains (8, 30, 31). This raises the possibility that a key factor in the bioactivity of agonists is the ability to partition into the microdomain where their target protein is located. Indeed it is well known that the 5HT$_{1a}$ receptor is modulated by cholesterol (11), and a recent study has shown that it partitions into cholesterol-rich lipid rafts (8). This is particularly pertinent for the agonists tested in this study because they too interact with cholesterol and so may preferentially partition into lipid rafts.

The system used here is a simplified model of the biological membranes within which the target proteins reside. However, the data show that molecules targeting the same protein can interact with a membrane in significantly different ways. Furthermore, some of the agonists tested interact more favorably with cholesterol than phospholipid components of brain lipid membranes. This in turn implies that some agonists may preferentially locate in cholesterol-rich lipid domains, where it has also been shown that the target protein is located. It also raises the intriguing possibility that the modulation of protein activity by the membrane is not exclusively through lipid/protein interactions but may also be due to lipid/drug interactions altering the location and orientation of the protein agonists. Further studies are underway to shed more light on the interactions between cholesterol and the 5HT$_{1a}$ used in this study.

Acknowledgment—We thank Prof. Clemens Glaubitz for stimulating and insightful discussions.

REFERENCES

1. Wiener, M. C., and White, S. H. (1992) *Biophys. J.* **61,** 434–447
2. Subczynski, W. K., Wisniewska, A., Yin, J. J., Hyde, J. S., and Kusumi, A. (1994) *Biochemistry* **33,** 7670–7681

3. Yau, W. M., Wimley, W. C., Gawrisch, K., and White, S. H. (1998) *Biochemistry* **37,** 14713–14718
4. Pinkus, A. G., and Custard, H. C. (1970) *J. Phys. Chem.* **74,** 1042–1049
5. Dougherty, D. A. (1996) *Science* **271,** 163–168
6. Castanho, M., and Fernandes, M. X. (2006) *Eur. Biophys. J. Biophys. Lett.* **35,** 92–103
7. Ramstedt, B., and Slotte, J. P. (2006) *Biochim. Biophys. Acta* **1758,** 1945–1956
8. Allen, J. A., Halverson-Tamboli, R. A., and Rasenick, M. M. (2007) *Nat. Rev. Neurosci.* **8,** 128–140
9. Siarheyeva, A., Lopez, J. J., and Glaubitz, C. (2006) *Biochemistry* **45,** 6203–6211
10. Scheidt, H. A., Pampel, A., Nissler, L., Gebhardt, R., and Huster, D. (2004) *Biochim. Biophys. Acta* **1663,** 97–107
11. Pucadyil, T. J., Kalipatnapu, S., and Chattopadhyay, A. (2005) *Cell Mol. Neurobiol.* **25,** 553–580
12. Villalain, J. (1996) *Eur. J. Biochem.* **241,** 586–593
13. O'Brien, J. S., and Sampson, E. L. (1965) *J. Lipid Res.* **6,** 537–544
14. Gross, J. D., Warschawski, D. E., and Griffin, R. G. (1997) *J. Am. Chem. Soc.* **119,** 796–802
15. Warschawski, D. E., and Devaux, P. F. (2005) *Eur. Biophys. J.* **34,** 987–996
16. Keller, R. (2004) *The Computer Aided Resonance Assignment Tutorial*, Cantina Verlag, Goldlau, Switzerland
17. Huster, D., Arnold, K., and Gawrisch, K. (1999) *J. Phys. Chem. B* **103,** 243–251
18. Deleted in proof
19. Forbes, J., Husted, C., and Oldfield, E. (1988) *J. Am. Chem. Soc.* **110,** 1059–1065
20. Polozov, I. V., and Gawrisch, K. (2004) *Biophys. J.* **87,** 1741–1751
21. Stamm, H., and Jackel, H. (1989) *J. Am. Chem. Soc.* **111,** 6544–6550
22. Holland, G. P., and Alam, T. M. (2006) *J. Magn. Reson.* **181,** 316–326
23. Gaede, H. C., Yau, W. M., and Gawrisch, K. (2005) *J. Phys. Chem. B* **109,** 13014–13023
24. Goni, F. M., and Alonso, A. (2006) *Biochim. Biophys. Acta* **1758,** 1902–1921
25. Wimley, W. C., and White, W. H. (1993) *Biochemistry* **32,** 6307–6312
26. Ollila, F., Halling, K., Vuorela, P., Vuorela, H., and Slotte, J. P. (2002) *Arch. Biochem. Biophys.* **399,** 103–108
27. Schiffer, M., Chang, C. H., and Stevens, F. J. (1992) *Protein Eng.* **5,** 213–214
28. Peroutka, S. J. (1986) *J. Neurochem.* **47,** 529–540
29. Millan, M. J., Rivet, J. M., Audinot, V., Gobert, A., Lejeune, F., Brocco, M., Newman-Tancredi, A., Maurel-Remy, S., and Bervoets, K. (1995) *J. Pharmacol. Exp. Ther.* **273,** 1418–1427
30. McIntosh, T. J., Vidal, A., and Simon, S. A. (2003) *Biophys. J.* **85,** 1656–1666
31. Lucero, H. A., and Robbins, P. W. (2004) *Arch. Biochem. Biophys.* **426,** 208–224
32. Leonard, A., Escrive, C., Laguerre, M., Pebay-Peyroula, E., Neri, W., Pott, T., Katsaras, J., and Dufourc, E. J. (2001) *Langmuir* **17,** 2019–2030